Chair:
Prof. Paola Taroni

DOCTORAL PROGRAM IN PHYSICS

The Doctoral Program in Physics at Politecnico di Milano aims at attracting bright students with good scientific background and clear interest towards development and applications of new ideas and technologies. It offers a wide range of opportunities in the fields of advanced applied physics, such as photonics and optoelectronics (lasers, ultrafast optics), biomedical optics (optical tomography), vacuum technologies (thin film depositions), material technologies (microelectronics and nanotechnologies, micromechanical processing), and advanced instrumentation (electronic and atomic microscopy, nuclear magnetic resonance).

Scientific education and training to develop general research abilities in all areas of applied physics is increasingly needed by advanced technological companies. Through a general education in the basic areas of applied physics and a specific knowledge in condensed matter physics, as well as optics and lasers, the PhD Program aims at the development of an experimental approach to problem solving techniques and at the attainment of a high level of professional qualification.

The Doctoral Program has strongly experimental character. The contents are strictly related to the research activities carried out in the laboratories at the Department of Physics. They can be divided into two main areas:

a. Condensed Matter Physics, including photoemission; spin-resolved electronic spectroscopy; magneto-optics; X ray diffraction; magnetic nanostructures for spintronics; synchrotron radiation spectroscopy, positron spectroscopy, semiconductor nanostructures.
b. Optics and Quantum Electronics, including ultrashort light pulse generation and applications; UV and X optical harmonics generation; biomedical applications of lasers; diagnostics for works of art; laser applications in optical communications; time domain optical spectroscopy and diagnostic techniques.

All research activities rely on advanced experimental laboratories located at Politecnico di Milano (Milano-Leonardo Campus and Como Campus) and are performed in collaboration with several international Institutions. Besides the experimental research, a consistent effort is devoted to the design and development of novel instrumentation.

The educational program can be divided into three parts: 1) Main courses specifically designed for the PhD program; 3) Activities pertaining to more specific disciplines which will lay the foundation for the research work to be carried out during the Doctoral Thesis; 4) Doctoral Thesis. The thesis work is the major activity of the Program. It has a marked experimental character, and will be carried out in one or more laboratories at the Department of Physics.
The students are also encouraged to perform part of their thesis work in laboratories of other national or foreign Institutions. Collaborations that may involve the PhD students are presently active with several national and international research and academic Institutions, such as: ETH-Zürich, EPL-Lausanne, Lund Institute of Technology, University of Paris-Sud, Ecole Polytechnique-Paris, University of Barcelona, University of Berkeley, University of Cambridge, Technical University of Wien, University of Bordeaux, Massachusetts Institute of Technology, Harvard University, INFM-CNR, IIT–Istituto Italiano di Tecnologia, European Space Agency, ENEA, Elettra-Ts, PSI-Villigen, Agenzia Spaziale Italiana, European Synchrotron Radiation Facility (ESRF-Grenoble).

The average number of fellowship/grants for students admitted to the PhD Program is twelve per year, while the average number of available positions is more than double. At present, the overall number of students in the three-year course is fifty-six.

Teaching and research activities of the Doctoral Program are controlled and organized by a number of Faculty members large enough to cover a wide spectrum of research fields. All members are highly qualified and active researchers. This ensures a continuous updating of the PhD program and guarantees that the students are involved in innovative work. A list of the Faculty members follows:

DOCTORAL PROGRAM BOARD		
Brambilla Alberto	Finazzi Marco	Ramponi Roberta
Ciccacci Franco	Ghiringhelli Giacomo	Stagira Salvatore
Cubeddu Rinaldo	Isella Giovanni	Torricelli Alessandro
D'andrea Cosimo	Lanzani Guglielmo	Taroni Paola
De Silvestri Sandro	Marangoni Marco	
Duò Lamberto	Nisoli Mauro	

The Doctoral Program relies also on the advice of a Steering Committee, formed by distinguished experts (see table below) coming from R&D industries or research laboratories, taking care that the goals of the PhD Program are in line with the needs of non academic world.

ADVISORY BOARD
Roberto Bez (NUMONYX, Scientific fellow - R&D)
Stefano De Rossi (Oerlikon Balzers Coating Italy S.p.A., General Manager)
Marco Grioni (EPFL - Lausanne, Professor)
Emilio Parisini (CNST - Fondazione Istituto Italiano di Tecnologia (IIT), Team Leader (Biochemistry))
B Hans von Känel (ETH-Zürich, Professor)

MAGNETIC TUNNELING JUNCTIONS FOR BIOSENSING AND ANTIFERROMAGNET-BASED SPINTRONIC DEVICES

Edoardo Albisetti - Supervisor: **Riccardo Bertacco**

Since the discovery of giant magnetoresistance in 1988 and its breakthrough application in data storage technology, magnetoresistive phenomena have been extensively studied and nowadays constitute the core of a variety of spintronic devices. Among them, magnetoresistive sensors in combination with magnetic markers are particularly suited for biosensing applications due their high sensitivity and ease of integration in compact lab-on-a-chip platforms.

This Ph.D. work deals with the realization and optimization of a biosensing platform based on magnetic tunneling junctions (MTJs), and on the development of novel spintronic devices comprising tunneling junctions whose magnetoresistance is governed by antiferromagnets, with no ferromagnets.

The starting point was the fabrication of MTJ-based sensor arrays by magnetron sputtering and optical lithography (Fig. 1). This task was carried out starting from the optimization of the single functional layers, up to the final integration of the microfabricated sensor chips with the microfluidic platform and with a multiplexed electronic setup for data acquisition. Our preliminary experiments on the detection of magnetic bead sedimentation led to the formulation of a new model for the sensor sensitivity to the magnetic markers, whose predictions were confirmed experimentally. Such model can be used for identifying the optimal working point on the sensor magnetoresistive curve, in order to maximize the sensitivity and reduce the limit of detection of the assays, as well as for realizing novel improved sensors starting from the design of their magnetic response.

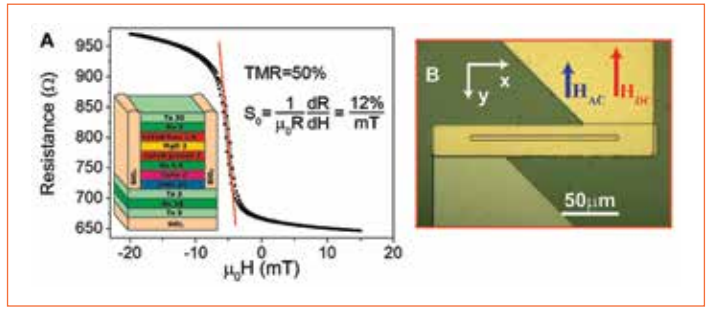

Fig. 1 A. Linear magnetoresistive curve of an MTJ. In the inset: structure of the MTJ grown by sputtering. B. Optical image of an MTJ.

The maximization of the sensor sensitivity was investigated also from the point of view of the spatial distribution of the magnetic beads on the sensor area. For addressing experimentally this issue in biomolecular recognition experiments, we developed a technique based on conventional optical lithography for creating micron-sized patterns of probe biomolecules such as single strand DNA. The detection of synthetic DNA hybridization events was successfully carried out both in conventionally functionalized and biopatterned sensors, showing a significant increase in the binding signal on biopatterned sensors, consistent with calculations (Fig. 2). Our biosensing platform was also employed for detecting natural *Hepatitis E* virus DNA, with the aim of realizing an integrated Lab-on-a-Chip platform for the point-of-care detection of pathogens in the agri-food industry.

MTJ-based sensors, due to their extremely high sensitivity to weak magnetic fields, are very promising for the study of the activity of neural cells *in-vitro* through the detection of the magnetic fields generated by ionic currents. In these studies, the control over the growth and orientation of neurons with respect to the sensor is fundamental to have a detectable signal. Such control can be achieved patterning gradients of extracellular matrix (ECM) proteins in correspondence of the sensors. With this goal, we demonstrated that thermochemical nanolithography (TCNL) can be used for patterning gradients of ECM proteins combining the high control over the protein concentration with nanometric resolution.

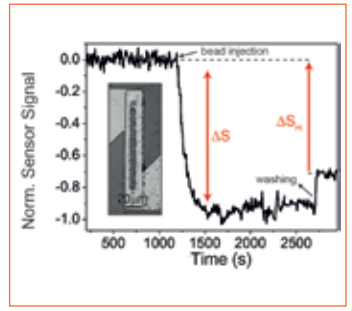

Fig. 2 Magnetic signal during a molecular recognition experiment. ΔSH is the binding signal. Inset: optical image of the sensor area after the experiment.

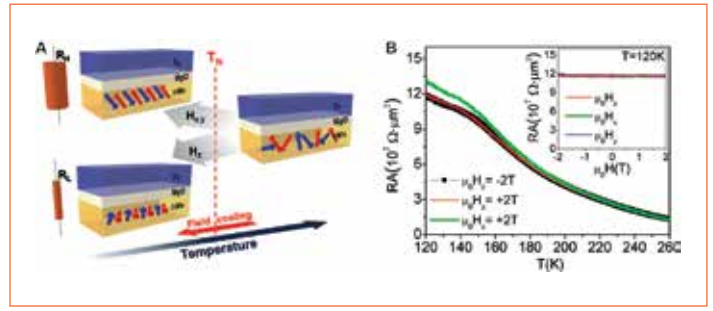

Fig. 3 A. 3D sketch showing the working principle of the device. B. Tunnel resistance data for field-cooling along z and x directions. The splitting of the two resistance traces, corresponding to the non-zero anisotropic magnetoresistance, is observed near T_N. Inset shows that the resistance remains constant when sweeping the field below T_N.

In parallel with the work on biosensing, the realization and studies on antiferromagnet-based tunneling junctions were carried out. The field of antiferromagnetic spintronics received a great boost with the demonstration of the first spintronic device whose transport is controlled by the tunneling anisotropic magnetoresistance (TAMR) in an antiferromagnet. Following this work, IrMn/MgO/Ta tunnel junctions (with no ferromagnetic materials) were fabricated in our group by sputtering and optical lithography. Field cooling experiments demonstrated the possibility to store magnetic information in such devices exploiting TAMR. In particular, two different metastable resistance states were reached performing field cooling across the Néel temperature of IrMn, with a different orientation of the applied magnetic field (Fig. 3). In perspective, such tunneling junctions can be the starting point for developing a new kind of thermally assisted MRAM devices based on TAMR in antiferromagnets.

EXPLORING LIGHT HARVESTING SYSTEMS VIA BROADBAND TRANSIENT PHOTOLUMINESCENCE SPECTROSCOPY

Marcelo J. P. Alcocer - Supervisor: **Dr. Annamaria Petrozza**

This thesis deals with the design, development and application of the ps-resolution broadband transient photoluminescence system at the Center for Nano Science & Technology in Milan. It describes the work performed predominantly by Marcelo J. P. Alcocer in the period 2011–2013 for attainment of his Ph.D.

The design, development and characterisation of the ps-resolution broadband transient photoluminescence system is presented. The system is shown to have almost unbroken spectral coverage in excitation from 280 nm to 1400 nm through the use of a commercial $Ti:Al_2O_3$ oscillator, second and third harmonic systems, and a custom-built frequency doubled optical parametric oscillator. Acousto-optical modulation permits excitation rates from 80 MHz to tens of kHz, whilst a custom-built confocal microscope allows three-dimensionally spatially resolved measurements to be performed down to a few microns. Separate streak camera and time correlated single photon counting detection systems are employed so as to provide unbroken coverage in the 300 nm to 2000 nm range, with a maximum system temporal resolution of ~1.9 ps for streak based measurements in the visible spectral region. A custom-built open source cross-platform software suite (trpl) for data visualisation and post-processing is also introduced.

Subsequently, in-depth investigations into the photo-physics of Rubrene (5,6,11,12-tetraphenyltetracene) single molecular crystals are presented.
The origin of previously observed spurious low-energy emission is shown to arise from an emissive state which is populated from the higher lying first singlet state. This low-energy state has a strong optical coupling to the ground state but exhibits remarkably weak absorption. Nevertheless, direct population from the ground state is demonstrated, thereby ruling out previous attribution to transient excited state species. It is speculated that the low-energy state originates from a low-density crystalline Rubrene-peroxide layer.
Investigations into the nature of the long-lived photogenerated species observed in Rubrene are also presented. Transient absorption and photoluminescence measurements are used to show that long-lived spectroscopic features previously attributed to triplet excitons arise in fact from polaron states. This finding undermines all previous direct spectroscopic observations of triplet excitons in Rubrene crystals, and so calls into question the significance and/or presence of the purported singlet fission and triplet fusion processes in Rubrene single crystals.

Finally, three case-studies are presented demonstrating the application of the developed transient photoluminescence system to investigations of a disparate array of material systems.

Firstly, the workings of a novel 'dye-doped' photovoltaic device architecture are elucidated through high temporal resolution transient photoluminescence measurements. A key energy transfer process from light harvesting antenna molecules (Spiro-TBT) to a co-polymer donor (PCPDTBT) is directly observed, and is subsequently shown to significantly improve device performance through spectral broadening.
Secondly, an investigation into the photo-protection mechanisms regulating photosynthesis in higher plants is presented. In this case, global analysis of bi-dimensional high temporal resolution photoluminescence data allows a new non-photochemical quenching mechanism to be identified. This mechanism is shown to take place in the photosystem I super-complex and be mediated by the light-induced accumulation of the xanthophyll zeaxanthin. Most interestingly, it is demonstrated that energy dissipation does not occur in the isolated light harvesting photosystem sub-units as expected, but rather only when they are bound to the corresponding photosystem core complex. This is markedly different to the situation in the better studied photosystem II counterparts.

Thirdly, two brief investigations into the promising new cation exchange route for nanocrystal synthesis are presented. Transient photoluminescence is used to confirm the successful completion of full cation exchange from CdSe/CdS dot/rod nanocrystals into corresponding ZnSe/ZnS nanocrystals. This opens the possibility of uniting the best of both material systems by projecting the good structural qualities of the Cd-based system onto less toxic Zn-based systems. Spectroscopic evidence for partial cation exchange from Cu deficient Cu-In-S nanocrystals to quaternary Cu-In-Zn-S nanocrystals is also presented, showing the potential of this approach for fine stoichiometric tuning of this up-and-coming material system.

STUDY OF ATTOSECOND ELECTRON DYNAMCIS IN DIELECTRIC NANOPARTICLES

Sunilkumar Anumula - Supervisor: **Mauro Nisoli**

High harmonic generation is the typical table top method employed to generate eXtreme Ultra-Violet (XUV) radiation in sub femtosecond time domain. This process is based on interaction of gaseous target with high intense ultrashort laser pulses. First train of attosecond (1as=10^{-18} sec) pulses are reported back in 2001 using this HHG process. From then onwards, several methods are being developed to isolate a single pulse from the train of pulses. However, the applications of these pulses are limited due to lower photon flux of these pulses (of the order of few pico joules).

My PhD work is involved in generation of higher energy isolated attosecond pulses (IAP) through polarization gating (PG) method. This is one of the ideal methods to obtain broadband isolated pulses. This method is based on confining the HHG process to half an optical cycle by modulating the polarization of driving laser field. However, Carrier to Envelope Phase (CEP) stabilized few optical cycle femtosecond Infra-Red (IR) pulses are needed to generate IAP through this polarization induced confinement. We implemented *hollow-core fiber compression* method in *differential pumping* configuration to obtain IR pulses with duration as short as *4 fs* with energy of *2.5 mJ* . With combination of these few optical cycle IR pulses and PG, IAP with energy of few *nJ* are generated. Shaded area in figure 1b., shows the continuous spectrum obtained through HHG process in *Kr*. Figure 1a., shows the variation of the XUV spectrum with CEP of driving laser field confirming the polarization induced confinement. Frequency resolved optical gating for complete reconstruction of attosecond bursts (FROG-CRAB) method is employed to characterize these pulses. These results confirm the pulse duration to be *250 as*.

These IAP along with CEP stabilized few optical cycle IR pulses are used for investigating ultrafast electron dynamics occurring in di-atomic molecules, biomolecules and nanoparticles. We measured the ultrafast electron dynamics in N_2 molecule initiated by attosecond pulses using V*elocity Map Imaging spectrometer* (VMIS). In particular a subcycle oscillatory dynamics related to quantum interference is investigated. We employed these IAP also to investigate charge migration, which plays a crucial role in fundamental biological mechanisms such as the transmission of biological signals in proteins and DNA. In particular charge migration mechanisms in *phenylalanine* and *tryptophan* are being investigated using *time of flight mass spectrometer*.

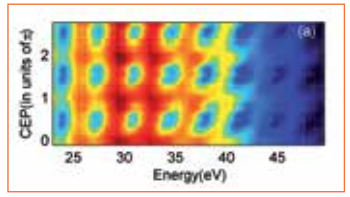

1a. Confirmation of the polarization induced confinement of the HHG process through few optical cycle IR pulses in Kr to obtain isolated attosecond pulses using polarization gating method.

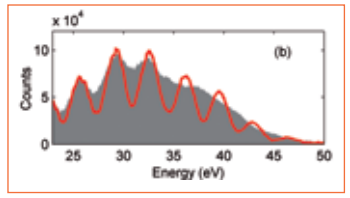

1b. Comparison the XUV spectra obtained at CEP value of zero (solid red line) and π/2(in shaded area) of driving laser field.

My thesis reports on the first pump-probe experiments in dielectric nanoparticles with attosecond temporal resolution. IAP are employed along with few optical cycle IR pulses to study electron dynamics in dielectric nanoparticles through streaking spectroscopy using *electron- time of flight spectrometer*(*e-TOF*). For this, nanoparticle beam is prepared from solution and focused to interaction region in time of flight (TOF) chamber using aerodynamic lenses. This nanoparticle beam source is developed by Prof. Kling's group from Max plank institute of Quantum Optics, Garching. Photoelectrons of the nanoparticles are recorded for different temporal delays between attosecond-XUV and IR pulses and a streaking spectrogram is constructed. Figure.2 shows the streaking spectrogram obtained in 95nm SiO2 nanoparticles. Modulation of the photoelectron distribution with periodicity of IR field's time period, confirms that photoemission and following transportation of the photoelectrons take place in sub femtosecond time domain. The measurements are performed on different sizes of SiO_2 nanoparticles and also extended to Al_2O_3, to study the dependence of the observed dynamics on chemical composition of the material. In streaking traces recorded with SiO_2 nanoparticles, a delay in the photoelectron distribution is observed along the XUV-IR temporal delay axis. The cut-off photoelectrons are shifted by *350 as* with respect to lower energy photoelectrons along the XUV-IR delay axis. This shift is linearly increased with the energy of photoelectrons with a slope of *32 eV/as*. Similar behaviour is observed even in case of Al_2O_3 nanoparticles with a larger amount of shift close to *420 as* between the distribution of the photoelectrons corresponding to *16 eV* and *27 eV*. This shift represents the delay between the instant of XUV photoionization and the instant these electrons leave nanoparticles. The observed delay in high energy photoelectrons is mainly due to higher number of collisions these photoelectrons undergo before leaving the nanoparticles after the XUV induced photoionization. This collisional motion of the photoelectrons observed in attosecond time scale open the possibility to explore the transport properties of a wide range of materials.

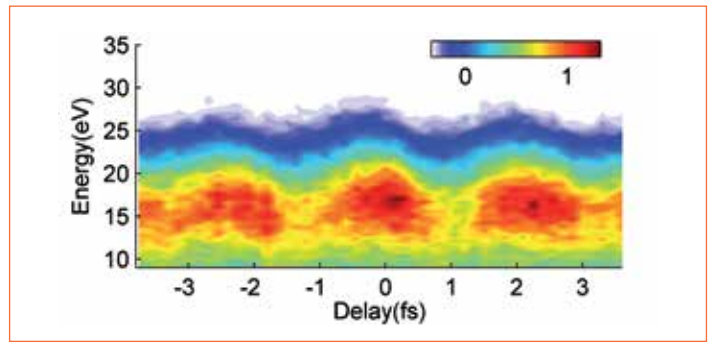

2.Streaking spectrogram recorded in 95 nm dielectric nanoparticles. Measurements are performed with step sized of 160 as. A shift of 350 as is observed in the phase of photoelectrons observed at 27 eV with respect to photoelectrons at 16 eV.

Second part of my thesis is focused on micro-focusing of attosecond pulses. An optical layout for obtaining aberration free micro-focused image with XUV radiation obtained by HHG process has been designed in collaboration with Dr. Luca Poletto, CNR, Padova, Italy. This design is based on grazing incidence toroidal mirrors to obtain a demagnification of 10. A new XUV-XUV beamline is built in our laboratory based on this layout. In order to achieve micro-focused image, optimal alignment of the toroidal mirrors is crucial. For this purpose, a *genetic algorithm* has been developed to obtain optimal alignment of the mirrors which are mounted on 6 axes stages. This new beamline with the genetic algorithm makes it possible to study electron dynamics in bio-molecules and other complex systems in sub femtosecond time domain.

INTEGRATED COMPLEMENTARY GRAPHENE INVERTERS IN ANALOG AND DIGITAL ELECTRONICS

Massimiliano Bianchi - Supervisor: **Roman Sordan**

The extremely high mobility of charge carriers in graphene at room temperature makes this material suitable for applications in high-speed electronics. GFETs exhibiting an over-unity intrinsic voltage gain are required for the realization of more complex graphene circuits and for this reason graphene voltage amplifiers were firstly investigated. They were obtained by using a very thin top-gate dielectric that allowed the realization of graphene complementary inverters, on single graphene flakes, with a high voltage gain (>10 dB) at room temperature. The AlO_x gate dielectric and the complete coverage of the channel increased the control over the charge carriers and eliminates the access resistances, allowing to reach high voltage gains A_v. This result reported the highest voltage gain obtained at room temperature for any kind of graphene amplifiers realized until that time.
Such graphene devices could be used as the main building block of both analog and digital electronics. However graphene cannot compete directly with conventional silicon CMOS logic inverters which are capable of reaching a voltage swing of 100% of the supply voltage, compared to 20% for the fabricated graphene devices. It is also difficult to reach a saturation region of the drain current in GFETs, in which the output conductance is minimized, allowing to have large voltage gains.
The fabrication of graphene amplifiers represents only the first step in the realization of realistic graphene digital circuits. The amplifiers were also used as digital logic gates at room temperature by applying the square-wave signal at the input. High values of the voltage gain in digital applications are required in order to distinguish between the two logic levels and to match the input and output signals. In this case it was not possible to obtain the matching between the input and output signals even though it was possible to distinguish the two logic levels. It was found that the mismatch between the signals is equal to the voltage at the Dirac point of the unbiased GFETs. Typically, charge neutrality points were far away from zero, showing a p-type doping in air, due to the adsorption of ambient impurities on graphene prior to the fabrication. In order to match the signals it was necessary to fabricate GFETs with Dirac points close to zero.
All fabricated graphene voltage amplifiers were realized using mechanically exfoliated graphene which is not a scalable technology. In order to solve the problem of the scalability

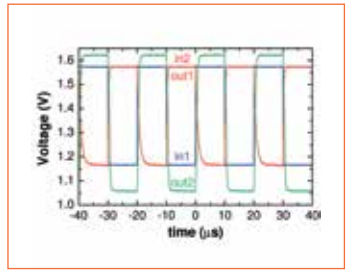

Fig. 1 Square-wave signals of two large-area graphene inverters in cascade connection measured under ambient conditions.

of complementary graphene inverters it was necessary to use large-scale graphene films grown by chemical vapor deposition (CVD). Graphene monolayers, provided by the group of Prof. Eric Pop from the Stanford University, where grown by CVD on Cu foils. They were transferred to SiO_2/Si substrates and integrated into graphene digital complementary inverters. Such a wafer-scale material allowed to achieved a weak saturation regime of the drain current and large voltage gain (A_v=-5.3). This is the highest gain reported for large-area monolayer graphene under ambient conditions in top-gated GFETs. It was demonstrated that by using GFETs with V_0<0.2 V in digital logic gates, with sufficiently large voltage gain, signal matching can be obtained. The voltage swing of the input and output signals was $V_{in,p-p}=V_{out,p-p}$=0.56 V . The same result was achieved even in GFETs with V_0>0.2 V but performing the measurement in vacuum. The lower pressure reduced only the voltage gain due to a different shift of the Dirac points of the GFETs that form the inverter. The fabricated graphene inverters were capable of reaching a voltage swing of 22.4% of the power supply, since GFETs cannot be turned-off in both logic states. Graphene logic gates could compete with high-frequency emitter coupled logic (ECL) gates in which the voltage swing is only 15% of the supply voltage. Replacing the typical materials that are used in the state-of-the-art of ECL gates with graphene, which has a higher mobility, it would be possible to reach even higher frequencies.
At the DC operating point that lies in between the highest gain points of two inverters (in which they exhibit $|A_v|$>4) the over-unity voltage gain is maintained in both inverters and as a consequence cascade connection can be realized, with the correct logic levels.
In this way it was possible to trigger one stage with another under ambient conditions (figure 1), a result that has never been achieved before at any temperature. This paves the way for the realization of realistic graphene digital circuits in which static power dissipation is not an issue. The very thin aluminum oxide layer allowed to reach the same oxide capacitance as in the 65 nm gate length Si CMOS which exceeds the typical oxide capacitance reported for graphene transistors.
The most important circuits in digital electronics are the ring oscillators (ROs) which are made by connecting an odd number of inverters so that the output of one inverter is connected to the input of the next inverter. ROs represent the perfect device to test the ultimate performances limits of a given technology. The previously demonstrated graphene logic gates were used in the realization of graphene ROs. This was the first demonstration of graphene digital integrated circuits operating at gigahertz frequencies, as shown in figure 2. It was also demonstrated that as the channel length of the GFETs in the ROs is reduced the capacitances and resistances of the channel are reduced and as a consequence f_O is increased. Reducing the parasitic capacitances and resistances it was possible to reach, at the channel length L=0.7 µm, a maximum oscillation frequency of 3.66 GHz. It was demonstrated that f_O only scales with 1/L even though both the resistance and the capacitance of the channel scale with L. This is because the

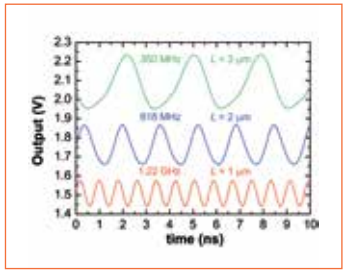

Fig. 2 Output signals of the best performing fabricated ring oscillators showing the best performances, measured for different gate lengths at the same supply voltage.

contact resistance (that scales with 1/W) and the parasitic resistances and capacitances of the interconnects do not scale.
It was found that the fabricated ROs exhibited even smaller gate delays compared to Si CMOS at the same gate length. Another advantage of graphene ROs was that they had a smaller sensitivity to the power supply fluctuations compared to silicon CMOS ROs.
Graphene digital circuits cannot directly compete with Si CMOS circuits due to larger power consumption. However, graphene could replace InP in high-frequency electronics due to its higher mobility but for this to happen further technological advances are needed.

ELECTRON SPIN PROPERTIES IN SiGe-BASED HETEROSTRUCTURES

Alberto Ferrari - Supervisor: **Prof. Franco Ciccacci**

The existing technology employed in modern electronics is gradually reaching the physical limits given by both the fabrication process and the design of devices. In fact, the more the size of components decreases, the more quantum effects become relevant, requiring increasingly sophisticated models to prevent and correct unexpected behaviors. For this reason, nowadays the new challenge consists in developing a new generation of devices able to overcome these limitations. Organic semiconductors, for example, would allow the fabrication of much smaller structures, but this technology is still at a very early stage. Instead of developing a completely new material, another option is to use different and more convenient physical properties of one already well known. This is the fundamental concept on which the relatively young field of spintronics is based. If we were to define this multidisciplinary branch of physics, we could state that "*spintronics involves the study of active control and manipulation of spin degrees of freedom in solid state physics*". In fact, in spintronics the electron spin represents the new carrier of information, which can replace the currently used electron charge, as in the case of the spinFET transistor, or otherwise the two can be used together in order to exploit new computational capabilities. Moreover, given the actual trend towards the integration of electronics, photonics and magnetism into multifunctional integrated devices, spintronics represents an ideal candidate to fulfill this task.

During my Ph.D. activity, I worked on this field of research, dealing mainly with optical injection of the electron spin polarization into group-IV semiconductor heterostructures. During the first two years, I took part in the development of a UHV system for spin-polarized photoemission measurements on both bulk-like and strained SiGe heterostructures. Upon excitation with circularly polarized light having a photon energy close to the semiconductor band-gap, a spin-polarized electron population can be generated in its conduction band, attaining values up to 50% spin polarization in bulk-like structures and up to 100% in strained ones.

We were able to lower the vacuum level of the system below the conduction band minimum at the Γ point of the Brillouin zone by employing $Si_{1-x}Ge_x$ alloys with a sufficiently

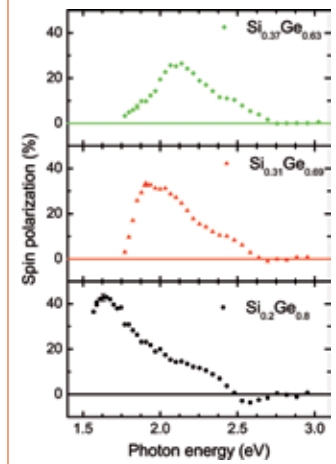

1. Electron spin polarization spectra at T = 120 K from $Si_{1-X}Ge_X$ alloys with x = 0.8, 0.69 and 0.63 (bottom, central, and top panel, respectively). The maximum value is found in the sample with x = 0.8, and it diminishes for lower Ge concentrations because of the photoemission of electrons from the conduction band minimum at L, where P ~ 0.

low Ge concentration. The subsequent polarization spectra are shown in Fig. 1, where it can be seen that the polarization maximum shifts according to the different energy band-gaps of the alloys and the maximum value of $P = 40\%$ is obtained in the one with a 80% Ge concentration.
Exploiting the 4% lattice mismatch between Si and Ge, in-plane compressively strained thin films were obtained by growing them on top of a SiGe substrate with a lower Ge concentration, in order to achieve much higher electron spin polarizations. As shown in Fig. 2, we measured a maximum spin polarization of about 62% in a strained pure Ge thin film and of about 72% in a strained SiGe alloy with a similar degree of in-plane compressive strain. This increase was due to the lowering of the sample vacuum level, which enabled photoemission exactly from the conduction band minimum at Γ, thus obtaining performances very close to those of III-V semiconductor strained alloys.

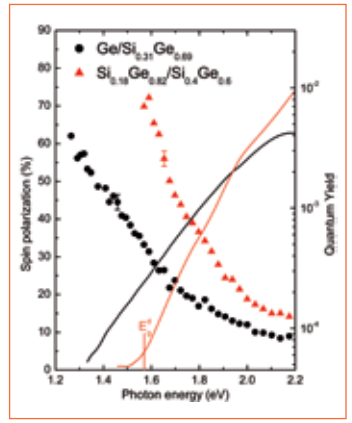

2. Electron spin polarization and quantum yield spectra at T = 120 K of the compressively strained Ge/$Si_{0.31}Ge_{0.69}$ and $Si_{0.18}Ge_{0.82}/Si_{0.4}Ge_{0.6}$ samples with their typical statistical error. E^d_g = 1.57 eV indicates the direct bandgap energy of the $Si_{0.18}Ge_{0.82}/Si_{0.4}Ge_{0.6}$ sample.

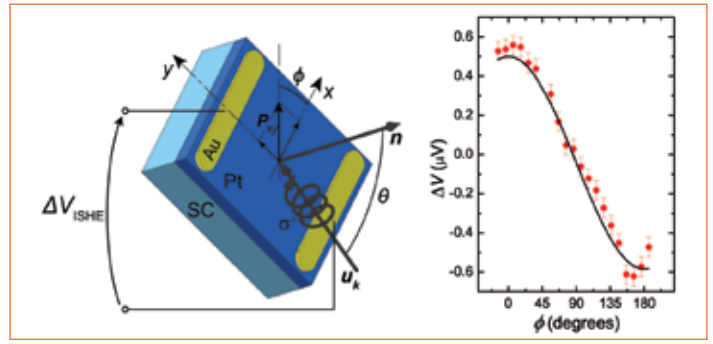

3. On the left, the experimental geometry is shown and in particular the angle ϕ in the sample plane between the direction of incidence of light and the x axis, perpendicular to the direction along which the voltage is detected. On the right, the ISHE voltage (red dots) is displayed as a function of the angle ϕ. The experimental data were taken at T = 300 K and are in good agreement with the expected cosine dependence (black curve).

Towards the end of the second year, we developeded a new system based on the inverse spin-Hall effect (ISHE) in order to achieve an electrical detection of the optically-injected spin transport and dynamics in Pt/Ge junctions. The spin-oriented electrons, generated at the direct gap of the semiconductor using circularly polarized light, provide a net spin current that yields an electromotive field $\mathbf{E}_{ISHE}$ in the Pt layer. This gives rise to a voltage signal, which is collected from two gold contacts evaporated at the edges of the Pt layer, as shown in Fig. 3, and measured by means of a lock-in amplifier. The same figure presents the measured signal as a function of the angle. In fact, an inversion is expected for opposite angles.
Finally, I spent five months at the CEA center in Grenoble in the "Nanostructure and Magnetism" group led by Prof. Matthieu Jamet. There we performed an electrical detection of the optically-injected spin signal through ferromagnet/semiconductor tunnel junctions realized with nanofabrication techniques.

OPTICAL PROJECTION TOMOGRAPHY: ADVANCED IMAGE ANALYSIS AND CONTRAST METHODS FOR DEVELOPMENTAL BIOLOGY

Luca Fieramonti - Supervisor: **Gianluca Valentini**

During the last decades, biological research has shown a great interest for the study of complex organisms and small animal organs in their entirety, by imaging their complete structure in 3D. Small animal models and embryos, typically studied in cancer research and developmental biology, fall in the so called mesoscopic scale (0.5-1.5 mm). As a result, imaging techniques able to visualize them in 3D within minutes are highly desirable.

Optical Projection Tomography (OPT) has been recently developed in order to perform tomographic, i.e. three-dimensional, visualization of mesoscopic samples. OPT is the optical analog of Computed Tomography. The sample is back-illuminated with visible light and the outgoing radiation is collected with a camera. The specimen is then rotated in order to capture several projections at different angular positions. Finally, mathematical reconstruction algorithms are applied to the set of projections, in order to obtain the virtual volume of the sample. However, attenuation and scattering properties of biological tissues limit the penetration depth of visible light, thus restricting applications of OPT to embryos and semi-transparent samples up to the millimeter scale. As a consequence, the use of chemical clearings is required to study bigger samples, preventing in-vivo experiments.

The present thesis is a report on the work done for extending OPT applications to *in vivo* mesoscopic organisms and for investigating new contrast mechanisms able to yield quantitative physiological information. As a result, new technical solutions for OPT and innovative image processing algorithms have been devised and implemented. The following OPT-based techniques have been mainly developed, though not exclusively, for a specific model organism, the zebrafish (*Danio rerio*), which has been chosen for its fundamental role in today developmental biology and cancer research.

Firstly, the thesis addresses the problem of photon scattering in OPT measurements on large samples, like adult zebrafish. Here, the scattering cannot be neglected, because it drastically reduces contrast and resolution. Tomographic imaging of adult zebrafish is useful, for example, in research studies about osteoporosis and bone loss diseases, because the skeletal system is thoroughly formed only at this stage. The scattering shown by non-cleared adult zebrafish creates heavy artifacts in the tomographic reconstruction, which prevent in vivo and time lapse measurements.

To counteract this problem, we developed and tested a particular version of OPT, called Time-Gated OPT (TGOPT). It uses second harmonic generation for selecting a limited temporal portion of a femtosecond light pulse that has passed through the diffusive sample. The scattering lengthens the optical path of the great majority of photons by changing their propagation direction, thus generating a blurring effect on the camera. Because of this, the pulse is broadened from the femtosecond to the picosecond scale. TGOPT is able to discriminate the photons that fall inside a 100 fs temporal window. Since the temporal window can be precisely placed on the leading edge of the signal pulse, TGOPT allows the detection of quasi-ballistic photons, for which the travel time in the sample is the fastest. Consequently, it rejects multiply scattered photons, which are responsible for blurring and resolution reduction in the acquired image. After validation, we were able to apply for the first time TGOPT to adult zebrafish, visualizing morphological details of the nervous and skeletal systems with a spatial resolution as small as 50 µm.
Successively, innovative contrast mechanisms have been developed for imaging specific biological organs.
In particular, we aimed to visualize the vascular network of zebrafish larvae *in vivo*. Indeed, tomographic reconstructions of the zebrafish cardiovascular system during embryo development is of paramount importance for understanding angiogenesis and vessel growth, which play a role also in pathological conditions like cancer.

We named the resulting technique Flow-OPT, since the contrast is given by the endogenous motion of blood cells inside vessels, without the use of fluorescent beads or staining. As a result, Flow-OPT opens the way to time lapse measurements on the same specimen and it gives the chance to follow angiogenesis *in vivo*. An image analysis algorithm extracts the position of blood cells in successive frames of the same view of the sample, while rejecting immobile structures. Then, blood cell motion is tracked to visualize the shape of the corresponding vessel. As a result, it is possible to get a vascular contrast image which shows only the vessels. By repeating the procedure at different angular positions of the sample and by applying OPT back-projection methods, the vascular network can be reconstructed in 3D.

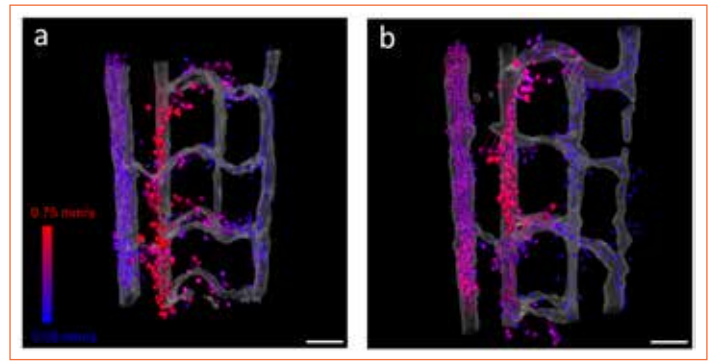

1. Blood velocity field comparison between zebrafish larvae at different development stages. (a) Velocity vector field of a 6 dpf zebrafish. (b) Velocity vector field of a 15 dpf zebrafish. Vessels are shown in gray. Scalebars are 50 µm.

Moreover, a specific particle image velocimetry algorithm, based on spatio-temporal correlation of pixel intensity, has been developed in order to quantify blood cell velocities inside vessels. This information, obtained on 2D images, is then converted in the actual 3D velocity vector with a custom algorithm implemented in Matlab (MathWorks). This procedure is called *optical vector field tomography* and it is able to visualize the complete velocity vector field over a large portion of the zebrafish trunk, superimposed to morphological information. The results obtained on zebrafish at different development stages are shown in Fig.1.

The last part of the thesis reports the development of correlative image analysis methods for selective plane illumination microscopy, which is another microscopy technique that, like OPT, has 3D imaging capabilities. This work has been carried out at the German Cancer Research Center, in Heidelberg, during about 6 months. In particular, a fluorescence correlation spectroscopy algorithm has been implemented in order to detect diffusion and direct flow of proteins inside human cancer cells.

In the future, all these techniques and image analysis algorithms will be further improved to decrease the measurement time, while increasing signal-to noise ratio. This would be helpful for *in vivo* applications and to follow zebrafish development from embryo to adult stage.

SILICON-GERMANIUM HETEROSTRUCTURES FOR SILICON PHOTONICS APPLICATIONS

Jacopo Frigerio - Supervisor: **Dr. Giovanni Isella**

Silicon photonics addresses the study and the technological application of silicon as an optical medium for generation, transmission, modulation and detection of light. It has been envisioned that silicon photonics will solve the interconnect bottleneck of CMOS technology, by the on-chip integration of silicon based optical interconnects with standard electronic elements. Monolithic germanium (Ge) based photonics have been regarded as one of the most promising options to realize active optical functionalities in Si CMOS compatible photonic circuitry. Despite being an indirect-gap semiconductor, the direct-gap optical properties of Ge have been extensively explored. Ge based devices have shown efficient optical modulation and photodetection within the telecommunication wavelength range in terms of both energy consumption and bandwidth. In particular, Ge/SiGe multiple quantum wells (MQW) have attracted much attention for the possibility to exploit Quantum Confined Stark Effect to realize high performance intensity modulators. The deposition of Ge/SiGe MQW cannot be performed directly on silicon because of the high lattice mismatch, which causes the accumulation of elastic energy in the MQW stack during the growth. When a certain critical thickness is reached, the elastic energy is released by the introduction of misfit and threading dislocations (TD), which are electrically active defects that can seriously deteriorate the crystal quality. For this reason, the MQW stack must be deposited on a SiGe virtual substrate (VS), with a Ge concentration close to that of the MQW. The VS, deposited on the silicon substrate, is carefully engineered in order to reduce the TD density to technologically acceptable values. One of the main problem to be addressed regarding Ge/SiGe MQW based modulators is their integration with other passive optical components such as waveguides. In the last years, many efforts have been made in order to find an efficient way to couple the MQW structure with silicon waveguides. In this work, a different approach based on the use of the virtual substrate as a low-loss waveguide is presented. Usually the VS is designed to have the same Ge content of the MQW stack in order to realize a strain-symmetrized structure in which the compressive strain in the Ge well is perfectly compensated by the tensile strain in the barrier. In such a structure, the VS has a high optical absorption coefficient at the modulation wavelength of the MQW stack, thus it is not suitable to realize a low loss waveguide. In this work, by choosing a suitable compositional mismatch between the MQW stack and VS, the optical loss in the VS at the modulation wavelength has been minimized, while maintaining a high crystal quality. We have grown 10 periods of 12 nm thick Ge wells and 16 nm thick $Si_{0.16}Ge_{0.84}$ barriers on top of a fully relaxed $Si_{0.16}Ge_{0.84}$ epilayer. The device was then processed by UV lithography and dry etching. The photonic interconnection is made by a Ge/$Si_{0.16}Ge_{0.84}$ MQW modulator connected to a Ge/$Si_{0.16}Ge_{0.84}$ MQW photodetector through a $Si_{0.16}Ge_{0.84}$ waveguide. The photocurrent in the photodetector is lower only by a factor three with respect to that of the modulator, and both devices have the same size. The waveguide related propagation loss is lower than 2 dB/cm at a wavelength of 1440 nm, and the optical insertion loss for the photonic interconnection is less than 5 dB at the same wavelength. The performances of the device are even slightly better than that reported for III-V devices bonded on silicon. Cut-off frequencies of 4GHz and 6.3GHz have been obtained for the detector and the modulator respectively. The measured bandwidth is RC limited. A photocurrent difference of 10 µA between the "0" and the "1" logic levels has been obtained by using 3V voltage swing at the modulator. The photodector, biased at -1V have shown a dark current of 10 nA, thus the shot noise is only 2.5 pA/$Hz^{1/2}$. The photonic interconnect thus has a very promising potential for low bit error rate data transmission. In conclusion, we have presented an experimental proof of concept integration of Ge-based photonic interconnection into planar optical circuitry on bulk silicon. The prototype shows that a Ge-rich $Si_{1-x}Ge_x$ VS can be used as a compact and low loss waveguide platform on which high quality epitaxial growth of the Ge-based optoelectronic devices can be directly performed.

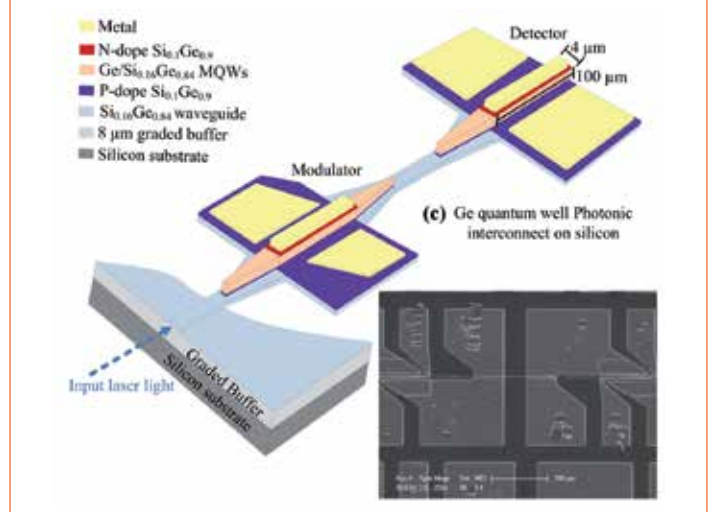

1. The fabricated photonic interconnect consisting of a Si0.16Ge0.84 waveguide integrated 4-µm-wide and 100-µm-long Ge/Si0.16Ge0.84 MQWs modulator and detector; the taper section is 55 µm long.

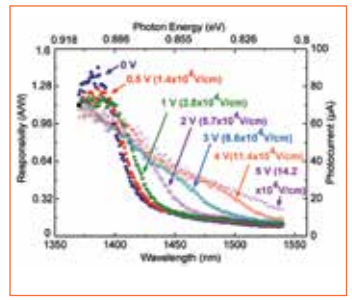

2. Photocurrent spectra obtained from transmission measurement at different bias voltages of the 4-µm-wide and 100-µm-long Ge/Si0.16 Ge0.84 MQW modulator.

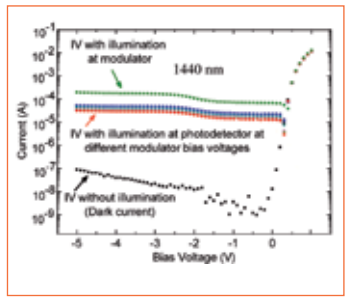

3. IV characteristics of the fabricated photonic interconnect.

EPITAXIAL GROWTH AND CHARACTERIZATION OF $Si_{1-x}Ge_x$ AND GaN CRYSTALS ON MICROMETER-SIZED SILICON PILLARS

Fabio Isa - Supervisor: **Dr. Giovanni Isella**

The stacking of different semiconductor layers has been widely investigated in the last decades both from the point of view of fundamental research and for the development of novel semiconductor devices. While most of the early works were focused on the integration of lattice-matched heterostructures, more recently, many efforts have been devoted to grow epitaxially mismatched heterostructures. Several devices, e.g. multiple-junction solar cells, photodetectors, high-brightness LEDs etc., require several micrometer thick epitaxial crystals. In particular, the epitaxial growth of dissimilar semiconductors on Si has a fundamental role in modern technology, it would enable the combination of semiconductor heterostructures with the well established CMOS technology. Whatever epitaxial growth technique is used, due to the misfit between the substrate and the epilayer lattice parameter, the system relaxes plastically at the growth temperature by introducing misfit dislocations. Unfortunately, misfit dislocations are terminated by threading dislocations which run through the whole crystal volume. Since threading dislocations strongly affect the performances of opto-electronic devices, many strategies have been proposed in the last years to reduce their density.

Despite the lattice stress is completely relaxed by means of misfit dislocations during the epitaxial growth, the crystal can be still strained at room temperature if its thermal expansion coefficient differ from that one of the substrate. The accumulated thermal stress can be deleterious, especially for thick epitaxial layers, by inducing wafer bowing and cracks, therefore compromising any possibility of further sample processing.

In this work we faced the problem of depositing on silicon substrates $Si_{1-x}Ge_x$ alloys, several micrometers thick, fulfilling the requirements of complete lattice relaxation, low threading dislocation density and absence of thermal cracks. In particular, our innovative epitaxial growth approach was based on depositing $Si_{1-x}Ge_x$ alloys on deeply patterned arrays of square micrometer-sized Si pillars.

The epitaxial growth was performed by LEPECVD. Thanks to its out-of-equilibrium growth conditions and partially isotropic distribution of the reactive impinging species, highly non conformal growth of Ge crystals, up to 50 µm tall and separated by few tens of nanometers, has been obtained. SEM images of the patterned Si substrate before and after the Ge deposition are respectively reported in Figure 1 a) and b).

We called this novel growth approach *3D heteroepitaxy*, which is based on self-limited lateral growth of the crystals. Firstly, the high deposition rate and low growth temperature ensure the surface adatom diffusion length being smaller than the Si pillar size and height, thus preventing material flow from the top to the bottom of the crystals. Secondly, steeper crystalline facets, close to the borders of the crystals, receive smaller reactive gas flux compared to the top ones. They suffer from reactive gas flux reduction due to shielding of neighboring pillars, thus further limiting their growth rate and lateral expansion.

The morphology and facet distribution of the crystals strongly depends on the competing growth velocities of each facet which can be finely tuned by changing the growth conditions.

The finite dimensions and the control of the top faceting of the crystals, allow to eliminate completely all threading dislocations at the lateral sidewalls, leaving the upper part of the crystals dislocation-free. Photoluminescence measurements performed on Ge crystals with different threading dislocation densities revealed that, in the case of dislocation-free 8 µm tall crystals, the inter-band PL signal is ~ 0.5 times that of a bulk Ge reference with fully comparable spectral shape. This result has been achieved for unintentionally doped Ge crystals without any annealing treatment. We also proposed a strategy to inhibit recombination of carriers at the defect sites by introducing fully strained $Si_{0.25}Ge_{0.75}$ reflectors within the Ge crystals, enhancing the ratio between the inter-band/dislocation PL recombination rate. We finally demonstrated the superior optical quality of dislocation-free Ge multiple quantum wells deposited on Si pillars compared to the best literature reference grown on graded buffer with threading dislocation density of ~10^6 cm^{-2}. High resolution X-ray nano-diffraction measurements, showed that Ge crystals are completely strain free. Indeed, finite element method simulations confirm that the tensile thermal strain is elastically released for Ge crystals with aspect ratio larger than ~ 1. While wafer bowing and thermal cracks are observed for thick Ge layers deposited on planar Si substrates, they are absent in the case of Ge crystals grown on micrometer-sized Si pillars. In the case of dislocation-free Ge crystals, their excellent crystal quality is confirmed by the FWHM of the (115) Bragg reflection peak which is comparable to that one of the silicon substrate.

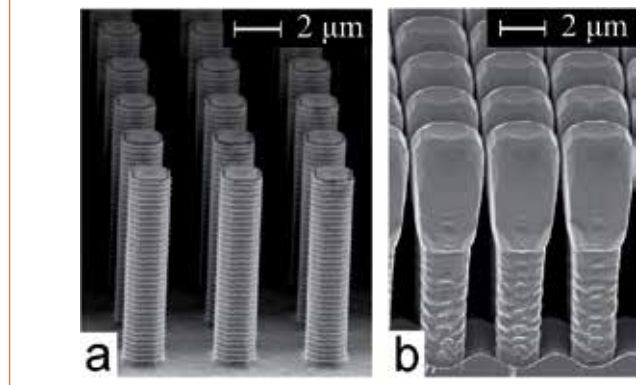

Figure 1: a) SEM image of the micrometer-sized patterned Si substrate. b) SEM image of a) after the deposition of 8 µm of Ge by LEPECVD.

We pursued a similar approach for another technologically relevant system: integration of GaN crystals on (001) silicon substrates by plasma-assisted MBE.

The novelty of our approach consists in depositing 2.5 µm of Si by LEPECVD on deeply patterned (001) silicon substrates, in this way crystals with large {111} facets were obtained. The {111} Si facets favor the deposition of the AlN buffer and GaN crystals. Indeed, after ~ 1 µm of deposition, GaN micro-crystals on {111} Si facets start to coalesce forming a continuous smooth layer, and after 3 µm the surface roughness has a RMS of 0.7 nm. Micro-photoluminescence and cathodoluminescence measurements confirm the high optical quality of the 3 µm thick GaN/Si crystals. Indeed, no yellow emission is detectable, while intense GaN bound exciton recombination, with a FWHM of 9.8 meV, takes place on the material deposited on the {111} Si facets. Moreover, most of the stacking faults recombination processes are located at the borders between different facets and in highly stepped surfaces.

We already have robust evidences that Ge crystals can be used to realize high efficiency IR light emitters and photodetectors, X-ray imaging detectors monolithically integrated onto a Si CMOS substrate and can act as virtual substrates for the deposition of III-As photovoltaic cells. Moreover, as already demonstrated here with the epitaxial integration of GaN/Si (001), and from unpublished results on SiC/Si, we strongly believe that once the conditions to have self-limited lateral growth are fulfilled, the use of micrometer-sized patterned Si substrates can be useful for the integration of several semiconductors on silicon, irrespective of lattice and thermal expansion coefficients mismacth, different polarity and crystal symmetry.

ULTRAFAST ENERGY AND ELECTRON TRANSFER PROCESSES IN NATURAL AND ARTIFICIAL LIGHT HARVESTING SYSTEMS

Margherita Maiuri - Supervisor: **Giulio Cerullo**

Almost 80% of global energy needs are satisfied by burning fossil fuels that are fated to deplete in approximately 100 years. Solar energy conversion provides a renewable and long-term solution for world's future energy consumption: ~0.05% of the energy provided by the sun would be sufficient to cover global needs. The question of how to exploit solar energy calls for novel concepts to harvest sunlight. Photosynthesis is the proof that organic materials can be strongly used to that purpose, so there is a growing interest in the design of manmade structures, inspired by Nature, that act as efficient light-harvesting devices (bio-inspired approach). Photosynthetic organisms rely on sophisticated pigment-protein complexes that play this function with an extremely high yield for light-to-charge conversion (>95%). The first step is the light harvesting (LH) process. Briefly, upon sunlight absorption, an electronic excitation is created in peripheral antennas of photosynthetic systems and it is rapidly transferred from outer antennas to the reaction center (RC) through a highly engineered network of complexes. The primary LH step occurs on extremely short, *femtosecond*, time scale suggesting that the speed of the process is intimately linked to its efficiency. Thus there is currently an intense experimental effort, in many research laboratories worldwide, aimed at understanding the early mechanisms that govern the LH processes in natural systems; this knowledge will be used to inform the design of artificial systems mimicking the natural ones.

In this Thesis we aim to shed light on the ultrafast energy transfer processes occurring in both Natural and Artificial LH-systems. To this regard, we have exploited ultrashort (sub *10fs*) optical pulses available in our laboratories to perform ultrafast non-linear spectroscopy. In particular *pump-probe* technique is a powerful tool to track ultrafast events, providing lots of information on the photoinduced dynamics of excited states in molecular systems.

In this framework, we first studied the ultrafast internal conversion process occurring in Carotenoids (Cars), which are ubiquitous pigments in LH systems. Cars play the fundamental role of photoprotectors but they act as light harvesters as well, helping the Chlorophylls in the sunlight collection. We time-resolve the photoinduced relaxation process in isolated Cars, completed in less than *200fs*, drawing an intricate scenario of the energy decay pathways. Our discoveries call for the inclusion of a new dark electronic state, strongly dependent on the environment and formed on sub-*30fs* timescale, in the excited state levels description.

Then, we focus on the energy transfer (ET) process in elementary photosynthetic organisms, named *purple bacteria*. They are excellent model systems as they rely on a small subset of molecules (Cars and bacterio-Chlorophylls (BChls)) for LH, placed in protein scaffold which stabilizes the configuration and tunes their electronic properties. We study the peripheral LH complex (LH2) from *Rps. Acidophila* purple bacteria, containing two main BChls, named B800 and B850 due to their absorption in the near-IR spectral range. We track the energy flow among different BChls within a time scale ranging from hundreds of *femtoseconds* to hundreds of *picoseconds*. In particular we time resolve the B800→B850 ET process, completed in less than *2ps*, and the subsequent relaxation of the B850 back to its ground state on a *ns* timescale. We also study the photosynthetic membrane of *Chr. Vinosum* bacterium, in which we follow the energy flow from LH2 to LH1 and the RC.

Next, we address the ET processes in Artificial bio-inspired light harvesting supramolecules. The attention is focused on the ET process in an antenna dyad, made of one Car and one porphyrin-like molecule, mimicking the BChl. We demonstrate that this system shows a promising quantum efficiency (around 40%), compared to the natural ones. We also describe the coherent (wavelike) electron transfer mechanism observed in triad system, made of a Car-porphyrin dyad linked to a fullerene molecule, thus mimicking a RC of the photosynthetic unit.

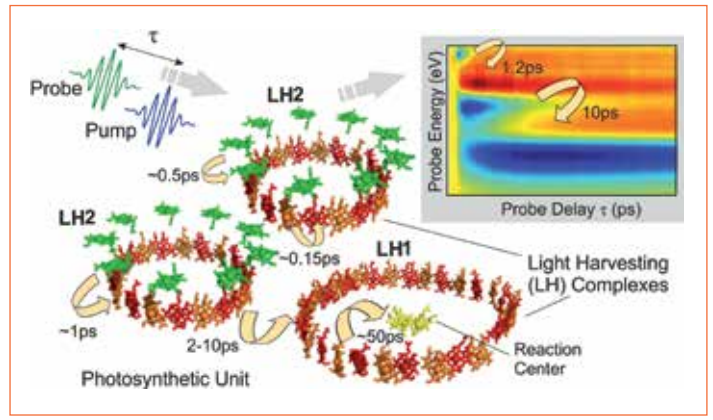

1. Cartoon of ET process and relative timescale in a photosynthetic unit of purple bacteria.

Following the category of artificial systems, a different approach to exploit the sunlight comes from photovoltaic (PV) technologies involving donor-acceptor systems able to harvest solar energy and use it to generate separate free charges for direct electric power (PV approach). Although photosynthetic and PV approaches share the first LH event, they work in a slightly different ways and give origin to different types of products: biomass or photochemical fuels in the case of photosynthesis, and electrical current in the case of PV. The dramatic progress in the performance of polymer-based solar cells (approaching more than 10% for organic devices) demands to elucidate the key phenomena governing the charge generation process. Our attention focuses on the basic charge separation occurring at the interface of an all organic-based donor/acceptor blend. We report the experimental results on a high efficient low-band gap polymer for advanced organic solar cells, addressing the role of excess energy in the hot dissociation process. Thanks to our ultrafast apparatus, we demonstrate that, upon excitation with excess photon energy, enhanced charge dissociation occurs via hot charge transfer mechanism in less than *30fs*. In this blend, charge generation could thus benefit from dissociation of a thermally excited charge transfer state, thus significantly enhancing the device efficiency.

The final part of the PhD work has been devoted to the realization and optimization of an innovative device, based on birefringent wedges, used to implement a powerful experimental tool, the bidimensional electronic spectroscopy (2DES). 2DES is the ultimate technique belonging to the non-linear spectroscopy class, since it measures both the real (absorptive) and imaginary (dispersive) parts of the complex third-order response. The main advantage, compared with the conventional pump-probe technique, consists in the spectral resolution delivered by 2DES, proving a means to disentangle congested spectra. This thesis reports preliminary results of 2DES spectroscopy used to study the electronic and energetic landscapes of the LH2 complex in purple bacteria, tracking the ET pathways among the intricate network of BChls.

DEVELOPMENT AND APPLICATIONS OF NONLINEAR AND TIME-RESOLVED MICROSCOPY TECHNIQUES

Egle Molotokaite - Supervisor: **Giulio Cerullo**

A subject of great interest in the physical and life sciences is the non-invasive characterization of mesoscopic objects within a complex heterogeneous system through optical microscopy. The goal is to achieve high spatial resolution with high sensitivity and chemical selectivity. Fluorescence microscopy is one of the possible techniques where the chemical contrast is provided by labelling with natural or artificial fluorescent probes. However, since chemical species or biological samples usually do not fluoresce themselves, the system of interest is being perturbed by introducing the fluorophores, which, besides the possible toxicity associated with staining, can also result in photo-bleaching, not to mention the additional complexity of the experiments. From another perspective, vibrational microscopy techniques allow non-invasive and label-free imaging. They rely on the inherent molecular vibrations which provide the natural chemical contrast. Infrared (IR) imaging and spontaneous Raman scattering imaging are two prevalent methods. While the former one is confined to the lower spatial resolution due to the longer wavelengths involved and suffers from water absorption, the latter is limited by the weak Raman scattering cross-section, which results in higher laser power and longer acquisition times.

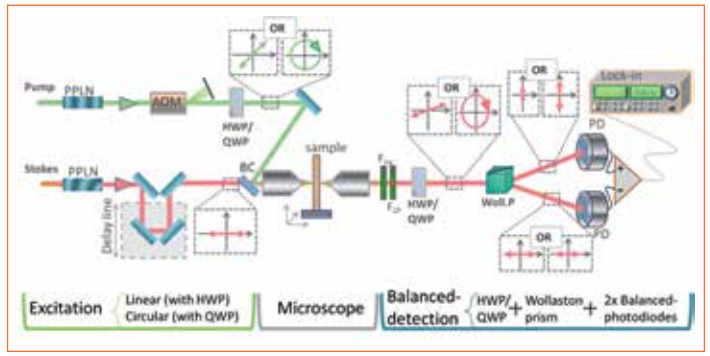

1 The experimental BD-RIKE setup; PPLN- periodically poled nonlinear crystal, AOM- acousto-optic modulator, BC- beam combiner, HWP/QWP – half-/quarter-waveplate, Woll.P- Wollaston prism, PD- photodiode.

Non-linear processes can significantly enhance the spontaneous Raman signal. As such, coherent Raman scattering (CRS) techniques provide several orders of magnitude higher sensitivity by using two laser beams, pump and Stokes, with frequency difference tuned to match the characteristic vibrational frequency of the molecule, thus making the molecular bonds to oscillate in phase and interfere constructively. Widespread applications of CRS techniques require laser excitation setups, composed of at least two synchronized pulse trains, with a possibility to tune the wavelength of each of them independently. In commonly used setups it is done by exploiting either two independent electronically synchronized solid state lasers or by a solid state laser and optical parametric oscillators(s) (OPOs), resulting in complex, bulky and costly setups.

One of the goals of my thesis was to develop the new technological approach for CRS microscopy based on spectral compression of femtosecond pulses emitted by a single amplified multiple-branch Er-fiber oscillator. Spectral compression is achieved by group-velocity mismatched second-harmonic generation in periodically-poled nonlinear crystals, and allows efficient synthesis of multiple synchronized narrow-bandwidth picosecond pulses with frequency difference continuously tuneable from 1000 to 3500 cm^{-1} and thus allowing to cover most of the biologically relevant vibrational frequencies. On the other hand, by taking advantage of the inherently broadband pulses generated by the highly nonlinear fiber, multiplex-CRS experiments can be performed. The system offers performances close to the current state of the art both for Coherent Anti-Stokes Raman Scattering (CARS) and for Stimulated Raman Scattering (SRS), but with significant advantages in terms of compactness and versatility.

Despite the growing recognition of CRS techniques, the most popular CARS and SRS are facing serious drawbacks, preventing them from the wider applications. In an attempt to overcome the limitations, we have developed a novel coherent Raman scattering technique - Balanced Detection Raman Induced Kerr Effect (BD-RIKE), whose setup is presented in fig.1. RIKE relies on the Raman induced birefringence in the sample, leading to polarization rotation of the Stokes field Es and to the creation of a field component ΔEs with perpendicular polarization. BD-RIKE technique combines the advantages of CARS, such as being linear-background-free, and advantages of SRS, including absence of non-resonant background, linear dependence on the concentration, self-heterodyne amplification. Furthermore, thanks to the possibility to measure both the imaginary and the real part of the nonlinear susceptibility, BD-RIKE gives direct access to the vibrational phase. Moreover, balanced-detection effectively cancels laser noise, allowing to achieve shot-noise limited detection. The advantages of BD-RIKE were discussed theoretically and proven experimentally. To demonstrate the potential of BD-RIKE microscopy, fig.2 shows the chemically sensitive imaging of the blend of polystyrene (PS) and polymethyl methacrylate (PMMA) beads in comparison with SRS technique under the same experimental condition. Further microscopic experiments were performed imaging human hepatocarcinoma cancerous cells, making BD-RIKE a promising technique in biological imaging applications. In addition, the same fiber-laser source has been used for time and space-resolved pump-probe experiments, providing a unique tool to study the dynamics of ultrafast relaxation processes in nanostructured materials. The complementary microscopic resolution can be extremely useful, especially for studying the nanoparticles, as it allows to measure the nonlinear time-resolved response from single particle, as well as heterogeneous samples, where the different molecular compounds are mixed, thus obtaining more precise information providing the link between the observed dynamical optical properties and the environment.

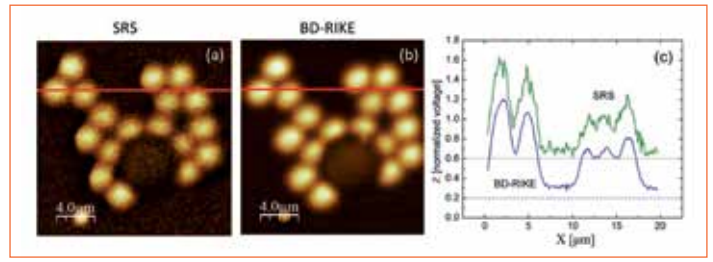

2. SRS (a) and BD-RIKE (b) images of a blend of PS and PMMA beads; (c) horizontal cuts along the red lines, showing the significantly better quality using BD-RIKE technique.

ELECTRIC FIELD CONTROL OF REMANENT STATES IN MAGNETIC AND FERROELECTRIC TUNNEL JUNCTIONS

Greta Radaelli - Supervisor: **Riccardo Bertacco**

Tunnel junctions consist of two metal electrodes separated by a very thin insulating barrier. Functional properties of tunnel junctions can be extended by using ferromagnetic materials as electrodes and/or ferroelectric ones as barrier, thanks to the tunnel magnetoresistance (TMR) and electroresistance (TER) effects. Tunnel junctions thus have great potential for application in real memory/logic devices, provided that room temperature switching between stable states can be controlled by an external electric field (E-field). This is a mandatory requirement in order to cope with the quest for higher storage density, higher speeds, and lower power consumption. The ultimate goal of the present thesis is to investigate memory/logic devices based on tunnel junctions which are characterized by (at least) two well defined remanent resistance states that can be controlled by an external E-field. To that purpose, two different strategies have been used: A) E-field control of the remanent resistance states of a magnetic tunnel junction by using magnetoelectric coupling (MEC) effects at multiferroic interfaces; B) E-field control of the remanent resistance states of a ferroelectric tunnel junction (FTJ) displaying TER effect. In the following are presented the main results and future prospects for each strategy. The first part of the thesis is devoted to the study of the physics of MEC at the fully epitaxial Fe/$BaTiO_3$ (BTO) interface. This knowledge is of fundamental scientific interest and should be valuable in view of the engineering of multiferroic heterostructures for application in electrically controlled spintronic devices. Fully epitaxial Fe/BTO bilayers have been grown in a multichamber system equipped with both pulsed laser deposition and molecular beam epitaxy. We show that in these fully epitaxial Fe/BTO systems, while strain-mediated MEC is suppressed likely due to clamping of BTO to the substrate, there is evidence for an undisclosed physical mechanism for interfacial MEC: the magnetization of the interfacial ultrathin oxidized iron layer (FeOx) can be electrically and reversibly switched on-off at room-temperature by reversing the BTO polarization thanks to the asymmetric effect that ionic displacements in BTO produces on the exchange coupling constants in the adjacent FeOx layer.
The second part of the thesis is instead devoted to the fabrication and characterization of FTJs whose remanent resistance states can be controlled by an electric field by exploiting the TER effect. Micron-sized FTJs have been fabricated on Pt/BTO/$La_{0.7}Sr_{0.3}MnO_3$ heterostructures grown on $SrTiO_3$(001) substrates by pulsed laser deposition and ex-situ sputtering techniques. These FTJ devices display two remanent resistance states that can be controlled electrically switching the ferroelectric polarization direction in the BTO barrier. TER ratios achieved in our large area junctions (up to 10^4%) represent up to now record values for room temperature TER in micron-sized FTJs without engineered interfaces. Moreover we show that integration in FTJs of half-doped manganites ($La_{0.5}A_{0.5}MnO_3$, A = Ca/Sr), intrinsically highly sensitive to external perturbations, is very promising to obtain an overall further enhancement of the TER effect.

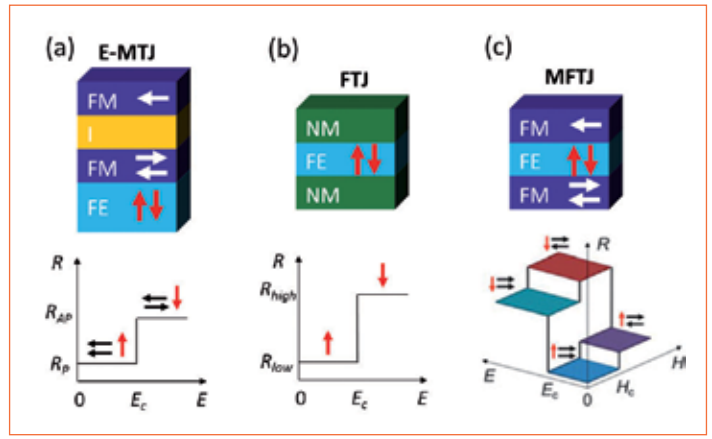

1: Schematic view of different types of E-field controlled memory/logic devices based on tunnel junctions: (a) E-field controlled MTJ (E-MTJ), (b) ferroelectric tunnel junction (FTJ) and (c) multiferroic tunnel junction (MFTJ). Ferromagnetic (FM), ferroelectric (FE), normal metal (NM), and insulating (I) layers are indicated where appropriate. Bottom panel show the resistance response of these junctions to magnetic (H) and electric (E) fields. Horizontal and vertical arrows indicate orientations of magnetization and electric polarization, respectively.

ULTRAFAST PROCESSES IN A STRONGLY COUPLED ORGANIC SEMICONDUCTOR MICROCAVITY

Sai Kiran Rajendran - Supervisor: **Tersilla Virgili**

Semiconductor microcavities have attracted interest not only due to their ability to modify the spontaneous emission rate of the emitter placed within, but also to form new cavity polariton modes when the cavity mode is in resonance with the exciton absorption in the regime of strong coupling. These cavity polaritons have a mixed excitonic and photonic character this has allowed observation of low-threshold polariton lasing and Bose-Einstein condensates in inorganic semiconductor based microcavities. However, due to the weak oscillator strength of Wannier-Mott excitons in inorganic semiconductors, cavity polariton states are observed mostly at cryogenic temperatures.
Frenkel excitons in disordered organic semiconductors like J-aggregates of cyanine dyes have oscillator strengths an order of magnitude higher and have shown Rabi splitting of 130meV even at room temperatures, showing the promise of achieving real-world polariton devices. In this work, we look at the ultrafast dynamics cavity polaritons in a strongly coupled cyanine dye J-aggregate microcavity (Figure 1(a)). All strongly coupled microcavities were fabricated by collaborators at the University of Sheffield. The J-aggregate was dispersed in a gelatin matrix sandwiched between two diffracting Bragg reflectors. The spacing between the two mirrors allowed the cavity mode to be sustained at 1.94eV at normal incidence. By angle tuning, the cavity mode could be brought into resonance with the J-aggregate absorption at 2.1eV. Anti-crossing (Figure 1(b)) of the polariton modes, characteristic feature of strong coupling, was observed in the dispersion plot.

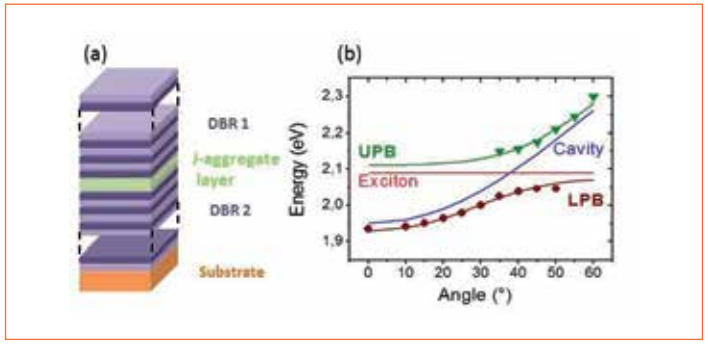

Figure 1: (a) Schematic of a microcavity on a fused-quartz substrate with diffracting Bragg reflectors (DBRs) made of alternate high and low refractive index layers and an active layer in the middle with the cyanine dye dispersed in gelatin matrix. (b)Typical dispersion relation of the polariton modes on angle tuning shows the upper polariton mode (green line) and the lower polariton mode (brown line) splitting when the cavity mode (blue line) is in resonance with the exciton absorption energy (red line) at 40° incidence.

In order to study the relaxation dynamics of the polariton states, ultrafast pump-probe spectroscopy was performed, at the Politecnico di Milano, using broadband 15-fs pump and probe pulses centered on 2.1eV generated from two non-collinear optical parametric amplifiers. Due to disorder in the organic material, a large number of J-aggregates are uncoupled to the cavity mode forming localized molecular excitations while only a small fraction form coherent polariton states. Hence this uncoupled exciton reservoir is expected to play a major role in the relaxation dynamics of the polariton states. Experimental confirmation for ultrafast relaxation of the upper polariton branch into the exciton reservoir, as well as relaxation from the excitons reservoir into the lower polariton branch by non-radiative scattering as the polaritons radiatively decayed out of the cavity obtained (Figure 2).

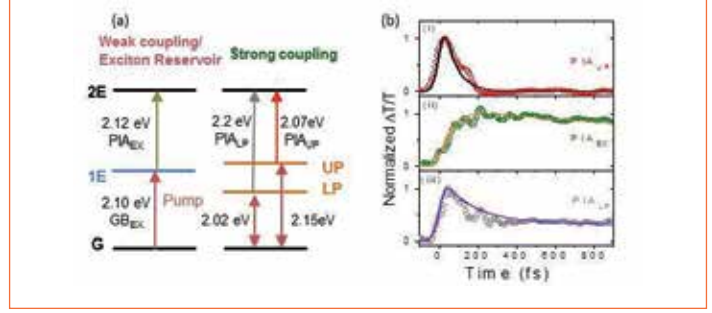

Figure 2: (a) Schematic of the energy levels showing transitions between the ground state (G), 1-exciton state (1E) and 2-exciton state (2E) in a weakly coupled cavity or the excitons reservoir(ER) with the 1E state splitting into the upper polariton branch (UP) and lower polariton branch (LP) at resonance. Dynamics of corresponding normalized photo-induced absorption transitions of the ER (PIAEX), UP (PIAUP) and LP (PIALP) are shown in (b) with the experimentally obtained data(empty circles) and modeled fits(solid lines).

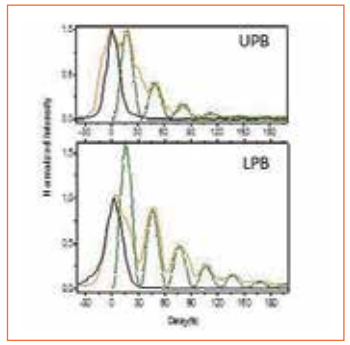

Figure 3: Time resolved transmission(orange lines) from the upper (above) and lower polariton branches (below) with 30 fs fit oscillations (green dotted line) beginning after the transmission maximum of the incident visible pulse(black line).

Observation of Rabi oscillations in the microcavity and the study of the coherence lifetime of cavity polaritons in the J-aggregate microcavity are also of interest to study the possibility of achieving polariton based devices. For a Rabi splitting of 135meV, 30 fs period oscillations between the polariton branches are expected as they exchange energies between their excitonic and photonic parts. Using ultrafast time-resolved up-conversion technique 7 fs broadband visible pulses centered on 590nm were incident on an angle-tuned microcavity. The coherent transmission of the polaritons through the microcavity was temporally resolved by using 14-fs near infrared pulses centered on 920nm as the gate pulse to form the sum-frequency generated spectra which showed 30 fs oscillations in the polariton transmission simultaneously reducing exponentially in a time of 50-70 fs as the polaritons decay radiatively (Figure 3). This value was also confirmed by another experiment-Spectral Interferometry at Carl von Ossietzky University of Oldenburg. Using broadband coherent white-light source, the beam was divided in the two equal parts using a beam splitter. The interference pattern formed by the two beams after one of them was transmitted through the microcavity was used to extract the phase induced in the fringes due to transmission through the strongly coupled microcavity. The complex spectral electric field was reconstructed using the amplitude and phase information and using an inverse fast fourier transform algorithm, the spectral response was converted to the temporal response of the electric field to show 30fs oscillations again in the microcavity transmission.

Photoluminescence (PL) studies of cavity polaritons were performed to observe non-linearities in the emission of strongly coupled J-aggregate microcavities. In our experiment, by pumping slightly above the J-aggregate absorption at 560nm, the PL was detected at different angles of incidence to show the dispersion of the lower polariton branch. Strongly coupled microcavities with two layers each of a different organic material were also studied. The idea is that one layer consisting of a 'pump dye' absorbs the pump light and its emission is reabsorbed by the second layer consisting of a thin film of cyanine dye. PL from these microcavities was also studied with increase in pump intensities.